

## EXPERIMENTAL TESTS OF TRANSPORT MODELS USING MODULATED ECH\*

J.C. DEBOO, C.M. GREENFIELD, Y.R. LIN-LIU, J. LOHR, T.C. LUCE, R. PRATER,  
D.P. SCHISSEL, G.M. STAEBLER, R.E. WALTZ  
General Atomics, P.O. Box 85608, San Diego, California 92186-5608

J.E. KINSEY  
Oak Ridge Associated Universities, Oak Ridge, Tennessee

E. FREDRICKSON  
Princeton Plasma Physics Laboratory, Princeton, New Jersey

R. BRAVENEC  
University of Texas at Austin, Austin, Texas

G.R. McKEE  
University of Wisconsin-Madison, Madison, Wisconsin

C.L. RETTIG  
University of California, Los Angeles, California

### Abstract

Both the dynamic and equilibrium thermal responses of an L-mode plasma to repetitive ECH heat pulses were measured and compared to predictions from several thermal transport models. While no model consistently agreed with all observations, the GLF23 model was most consistent with the perturbed electron and ion temperature responses which may indicate a key role played by electron modes in the core of these discharges. The IIF and MM models performed well for the electrons while the IFS/PPPL model agreed with the ions.

### 1. INTRODUCTION

Simulations have shown that perturbative transport experiments, where the dynamic plasma response is probed, can provide a more sensitive test of transport models compared to a comparison of measured and simulated temperature profiles from a power balance analysis. A perturbation source that deposits heat locally into the plasma particle species under study is preferred. Experiments have been performed on the DIII-D tokamak using modulated ECH as the perturbative heat source with the resonance layer off axis. The electron and ion response to the perturbation is measured and the amplitude and phase of the perturbations and the unperturbed temperature profiles are compared to predictions from several transport models.

### 2. TARGET PLASMA

To avoid inherent plasma perturbations such as sawteeth and ELMs, an MHD quiescent discharge in an L-mode configuration, limited on the inside wall of the vacuum vessel (Fig. 1), was chosen as the target plasma with a plasma current of 0.8 MA and electron density of  $2\text{--}2.5 \times 10^{19}\text{m}^{-3}$ . Early in the discharge, 4 MW of neutral beam power was applied to produce a sawtooth-free period during which 1.1–1.3 MW of ECH was applied in 20 ms pulses every 40 ms (Fig. 2) for a duration of 1 s. From 60%–75% of the total ECH power applied was in the X-mode with the remainder of the power in the O-mode. The X-mode power is calculated to be strongly absorbed during the first pass through the ECH resonance layer. Since the single pass absorption of the O-mode is low and the vessel walls are good reflectors, in the following simulation studies the O-mode power was assumed to be uniformly distributed along the vertical ECH resonance line through the plasma (Fig. 1). The ECH power was directed into the vessel so as to have the first pass absorption near the midplane of the vessel, which meant that the O-mode power was deposited no closer to the center of the plasma than

---

\*Work supported by U.S. Department of Energy under Contracts DE-AC03-89ER51114, DE-AC02-76CH03073 and Grant Nos. DE-FG05-96ER54346, DE-FG02-92ER54139, and DE-FG03-86ER53225.

the X-mode power. This was a necessary arrangement since the focus of the experiment was on the propagation from the off-axis deposition toward the plasma center. A toroidal field of 1.67 T resulted in second harmonic ECH power absorption ( $f_0 = 110$  GHz) at a normalized plasma radius  $\rho_{\text{ECH}} = 0.24\text{--}0.32$ . In order to probe more of the plasma two additional cases with ECH resonant layers at  $\rho_{\text{ECH}} = 0.4$  and  $0.5$  were obtained by varying the launch angle of the ECH power and the toroidal field. The unperturbed profiles for each of the three deposition locations were very similar with the  $\rho_{\text{ECH}} = 0.3$  case having a slightly lower density which resulted in slightly more peaked temperature and toroidal rotation profiles. Plasma impurity content was dominated by carbon, resulting in  $Z_{\text{eff}} = 2$  in the plasma core.

### 3. PLASMA RESPONSE TO ECH

The ECH heat pulse produced perturbations up to  $\delta T_e \sim 200$  eV at the resonant layer for the case with  $\rho_{\text{ECH}} = 0.3$ , observed by monitoring electron cyclotron emission (Fig. 2). The pulse shape is consistent with integration of the applied heat pulse with some deviation from a linear rise due to transport during the heat pulse. The thermal energy confinement time for these discharges is 30–45 ms. The electron perturbation rapidly propagated to the plasma core with little phase shift while the amplitude was reduced to  $\sim 30$  eV. The ion temperature decreased in response to the electron heat pulse and the amplitude of  $\delta T_i$  increased as the perturbations propagated to the plasma core, in contrast to a decrease in  $\delta T_e$ , reaching values up to  $\sim 200$  eV for the case with  $\rho_{\text{ECH}} = 0.3$ . Fourier analysis of charge exchange recombination radiation indicated the ion temperature response at the resonant layer is  $\sim 180^\circ$  out of phase with the electron response (Fig. 3) and also rapidly propagated to the plasma core, maintaining its out of phase relation to  $\delta T_e$ . It is important to note that the time scale for collisional transfer of energy between the perturbed electrons and background ions is several hundred milliseconds, long compared to the ECH modulation period, and hence changes in the ion temperature occur due to changes in the ion thermal diffusivity rather than changes in source terms of the ion power balance. Power balance in these discharges is achieved by each species predominantly conducting away the neutral beam and average ECH power deposited.

The amplitude of density fluctuations was modulated by the ECH pulses. Measurements were taken at low  $k$ , below  $3\text{ cm}^{-1}$ , with a beam emission spectroscopy diagnostic (BES) and at higher  $k$ , near  $12\text{ cm}^{-1}$  with a far infrared (FIR) scattering diagnostic. For a discharge with  $\rho_{\text{ECH}} = 0.7$ , the amplitude of fluctuations measured by the BES system near  $\rho_{\text{ECH}}$  exhibited a 15% peak-to-peak modulation in phase with the ECH pulses while outside of  $\rho_{\text{ECH}}$  little or no modulation was observed. Modulation of the fluctuation amplitude at  $\rho = 0.7$  with heating at smaller values of  $\rho_{\text{ECH}}$  was not observed, possibly due to smaller  $\delta T_e$  values produced at  $\rho = 0.7$ . The poloidal velocity of these

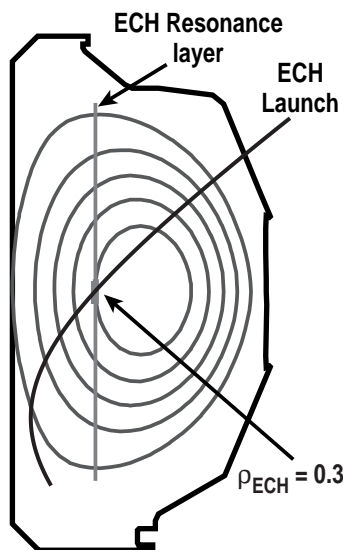


FIG. 1. Equilibrium flux plot of L-mode discharge. The first pass ECH absorption region is near the midplane of the vessel. Cases with  $\rho_{\text{ECH}} = 0.3, 0.4$  and  $0.5$  were studied.

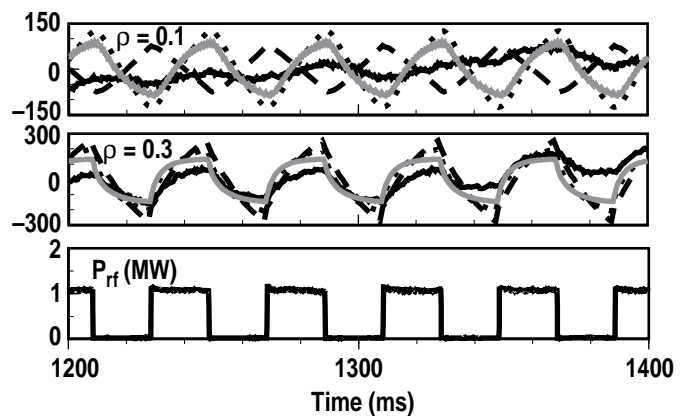


FIG. 2. Perturbed electron temperature,  $\delta T_e$  (eV), at  $\rho = 0.3$  and  $\rho = 0.1$  for measured data (solid, black lines), and simulated data from the IFS/PPPL model (dashed lines), IIF model (dotted lines), and GLF23 model (solid, grey lines).

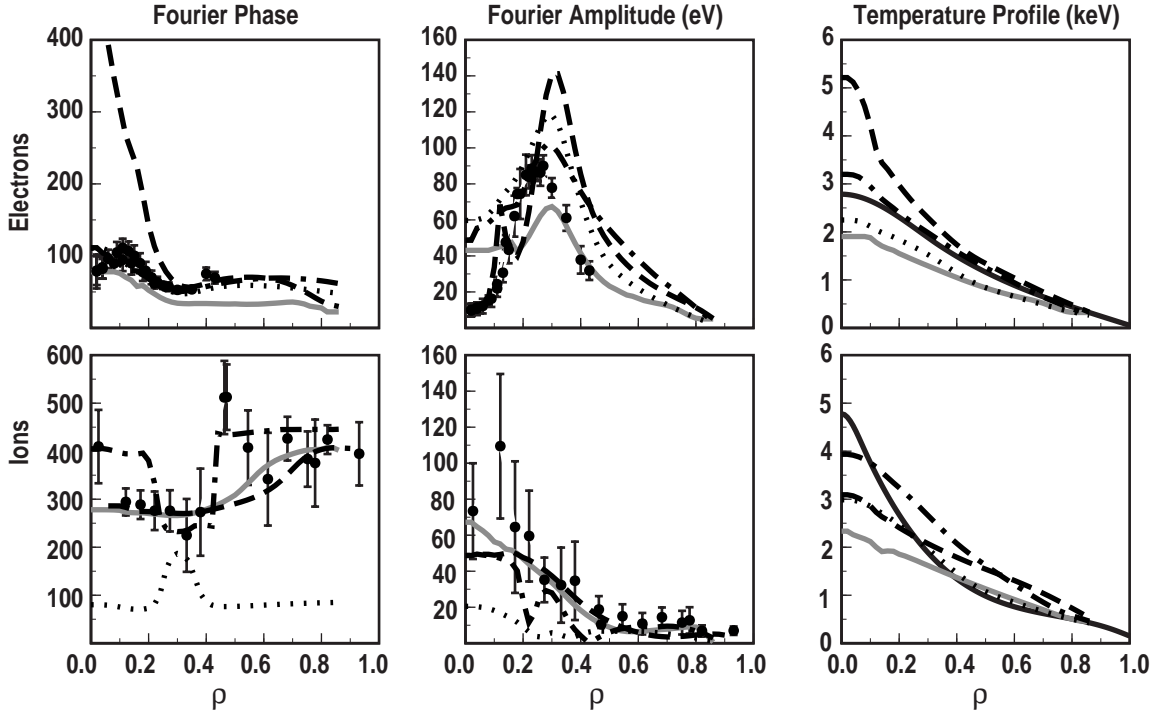


FIG. 3. Fourier analysis of phase and amplitude for  $\delta T_e$ ,  $\delta T_i$ ,  $T_e$ , and  $T_i$  for measured data (circles), IFS/PPPL model (dashed lines), IIF model (dotted lines), MM model (dot-dashed lines), and GLF23 model (solid, grey lines).

fluctuations was modulated out of phase with the ECH pulses. This observation is consistent with previous experiments where application of ECH produced a slowing of plasma toroidal rotation and a reduction in radial electric field  $E_r$  since the poloidal velocity of the fluctuations is proportional to  $E_r$  in the absence of large diamagnetic flows, as expected for these discharges. Modulation of larger  $k$  fluctuations was not observed with the FIR system. Modeling of this turbulent fluctuation behavior has begun and preliminary results have been reported [1].

#### 4. COMPARISON TO MODEL SIMULATIONS

Several theoretical and empirical models for describing electron and ion thermal transport have been examined. Two models which represent extremes in stiffness, a strong dependence on temperature gradients, are the IFS/PPPL model [2] based on ion temperature gradient (ITG) mode turbulence which depends sensitively on a critical temperature gradient and the Itoh-Itoh-Fukayama (IIF) model [3] based on current diffusive ballooning mode theory which has no critical temperature gradient dependence. The GLF23 model [4] contains essentially the same ITG physics model as does the IFS/PPPL model plus ETG modes and trapped electron (TEM) modes. The Multi-Mode (MM) model [5] also contains ITG and TEM modes but has no ETG modes and includes drift-resistive and kinetic ballooning modes. Simulations of the electron and ion temperature profile response to the ECH perturbative heating were performed with these models using a time-dependent transport code, MLT. Only thermal heat transport was considered and the temperature profile boundary conditions were taken from experimental measurements at  $\rho = 0.9$ . The electron density profile was held fixed at the steady-state experimentally measured level. The simulations were progressed in time until the predicted oscillatory perturbations about an equilibrium value were clearly determined. Fourier analysis was then applied to the prediction from each model and compared to the fourier analysis at the fundamental frequency of the electron and ion temperatures experimentally measured across the plasma. Fourier analysis significantly enhances the visibility of small amplitude perturbations immersed in a noisy background and was particularly necessary to clearly discern the experimental  $\delta T_i$  perturbations.

The ITG-based models agree with the electron and ion temperature profile response at the ECH resonance layer. For these models, the  $T_i$  response is largely determined by the effect of the  $T_i/T_e$  ratio on the ITG mode threshold. As the electrons are heated at  $\rho_{\text{ECH}}$ ,  $T_i/T_e$  decreases which in turn destabilizes the ITG-driven transport and thereby increases the ion transport at that location. This behavior is consistent with the decrease in  $T_i$  observed in response to the electron heat pulse and with

the increased density fluctuations observed with BES. The experimental amplitude of  $\delta T_e$  decreases while  $\delta T_i$  increases as the pulse propagates toward the plasma core (Fig. 3). Each of the models was capable of reproducing this particular trend. The models containing ITG modes most closely reproduced the amplitudes of  $\delta T_i$ .

The predicted phase of  $\delta T_e$  and  $\delta T_i$  in the plasma core proved to be the most sensitive test for differentiating between the models. Only the GLF23 model is in reasonable agreement with the phase behavior of both  $\delta T_e$  and  $\delta T_i$  for the  $\rho_{ECH} = 0.3$  case shown in Fig. 3. Agreement with electrons is poorer for the other cases studied; predicted phase shifts are smaller than measured in the core. The IFS/PPPL (MM) model describes the ion (electron) phase well however it incorrectly predicts a  $\sim 180^\circ$  phase shift in  $\delta T_e$  ( $\delta T_i$ ) as it propagates inward from  $\rho = 0.3$  to  $\rho = 0.1$  whereas the experimental result exhibits only a small phase shift. The IIF model describes the observed electron phase behavior well but incorrectly predicts that the ion pulse remains roughly in phase with the electron pulse near the plasma core. The IIF model is the only model which does not predict the  $\sim 180^\circ$  phase shift in  $\delta T_i$  observed as it propagates outward from  $\rho = 0.4$  to  $\rho = 0.6$ .

The magnitude and shape of the unperturbed, equilibrium temperature profiles are generally not well described by any of the models, with rms errors typically exceeding 20%. The shape of the  $T_e$  profile is reasonably well described by all but the IFS/PPPL model. The magnitude of  $T_e$  for GLF23 and IIF is somewhat low in the case shown in Fig. 3 and worse in other cases. The MM model predicts  $T_i$  well for the other cases studied but the shape for the case shown in Fig. 3 is not well matched. The magnitude and shape of  $T_i$  is well described by the GLF23 and IIF models only for  $\rho \geq 0.4$ . The predicted central values of  $T_i$  and  $T_e$  can be better matched with the GLF23 model, without significantly changing the predicted perturbed amplitude or phase, by including E×B flow shear stabilization [6]. However, the mismatched shape of the  $T_i$  profile is not improved by E×B flow shear. Experimental measurements of toroidal and poloidal rotation velocities which allow a comparison of shearing rates with maximum linear growth rates indicate that low k ITG and TEM modes are marginally stabilized in these discharges while the ETG modes at larger k values remain unstable. While including E×B flow shear in the IFS/PPPL model can improve the agreement with  $T_i$  in the core, predicted core  $T_e$  values become much too large. Since there are no ETG or TEM modes included in the IFS/PPPL model, the diffusivity drops to the neoclassical level when the ITG modes are stabilized.

The issue of the sensitivity of predicted perturbed results to the equilibrium temperature profiles has not been addressed in the initial analysis presented here. The extent to which the measured equilibrium  $T_e$  and  $T_i$  profiles are not reproduced by a given model may impact the model predictions for  $\delta T_e$  and  $\delta T_i$ . However, as mentioned above, comparison of the GLF23 analysis with and without E×B shear stabilization indicated that significantly different equilibrium profiles did not result in significant differences in predicted  $\delta T_e$  and  $\delta T_i$  values.

## 5. SUMMARY AND CONCLUSIONS

The overall observations indicate that the electron and ion responses to the ECH perturbation are out of phase with each other at the plasma core and at the resonance layer. Only the GLF23 model predicts this general characteristic at the plasma core which could indicate that electron modes, particularly ETG modes which are unique to the GLF23 model and calculated to be unstable, may be playing a key role in the heat transport near the core of these discharges. Since the electron and ion phase response to the heat pulse was very different it seems unlikely that a single fluid transport model will be capable of describing this behavior. The single fluid IIF model and the MM model described the electron behavior reasonably well in all cases studied but not the ion behavior while the IFS/PPPL and GLF23 models described the ion behavior reasonably well in all cases studied. Only the GLF23 model was in reasonable agreement with both electrons and ions for the case with  $\rho_{ECH} = 0.3$ . The overall results of these experiments remain a challenge for any one individual model to describe well.

## REFERENCES

- [1] BRAVENEC, R., *et al.*, to be published in Proc. 25th EPS Conf. on Controlled Fusion and Plasma Physics, Prague, Czech Republic, 1998.
- [2] KOTCHENREUTHER, M., *et al.* Phys. Plasmas **2**, 2381 (1995).
- [3] ITOH, S.I., *et al.*, Phys. Rev Lett. **72**, 1200 (1994).
- [4] WALTZ, R.E., *et al.*, Phys. Plasmas **4**, 2482 (1997).
- [5] KINSEY, J.E., *et al.*, Phys. Plasmas **3**, 3344 (1996).
- [6] BURRELL, K.H., Phys. Plasmas **4** 1499 (1997).